New Physics: Sae Mulli,
Vol. 69, No. 2, February 2019, pp. 136∼141
http://dx.doi.org/10.3938/NPSM.69.136

Magnetothermal Properties of Triethylene Glycol-Coated Cobalt-Zinc-Ferrite Nanoparticles for Magnetic Hyperthermia Applications

Ashfaq Ahmad · Hongsub Bae · Ilsu Rhee*
Department of Physics, Kyungpook National University, Daegu 41566, Korea

(Received 8 November 2018 : accepted 14 December 2018)

Cobalt zinc ferrite ($Co_{0.6}Zn_{0.4}Fe_2O$) nanoparticles were synthesized using a one-step hydrothermal method. Triethylene glycol (TREG) was used as a biocompatible coating material. The TREG-coated nanoparticles were spherical, with an average diameter of 9.82 nm. The Fourier-transform infrared spectra confirmed the presence of a TREG-coating on the surfaces of the nanoparticles. The particles had a saturation magnetization of 84 emu/g and a coercivity of 32 Oe. The heating capability of the particles was evaluated using an induction system, and the heating curves for aqueous samples with various particle concentrations were obtained. An alternating magnetic field with an amplitude of 4.5 kA/m and a frequency of 216 kHz was applied to the samples. The optimal particle concentration in water for achieving the hyperthermia target temperature of 42 °C was 4.58 mg/mL. The specific absorption rate (SAR) of the 2-mg/mL sample was 83 W/g. The linear relationship between the SAR and the square of the field strength was confirmed for a representative 10-mg/mL sample. These findings show that TREG-coated particles are suitable for magnetic hyperthermia applications owing to their superparamagnetic properties and high SAR values.

PACS numbers: 75.20.-g, 61.46.-w, 61.46.Df
Keywords: Zinc-doped cobalt-ferrite nanoparticle, Triethylene glycol coating, High specific absorption rate

I. INTRODUCTION

Magnetic nanoparticles, in particular, ferrite nanoparticles, have been extensively studied owing to their potential for application in various fields including high-density information storage systems [1], gas sensors [2], magnetocaloric refrigeration [3], magnetic resonance imaging [4,5], medical diagnostics [6], drug delivery, and magnetic hyperthermia [7,8].

Cancer cells are more susceptible to heat than healthy cells owing to their inefficient release of heat; this property of the cancer cells is used in magnetic hyperthermia [9]. Magnetic nanoparticles generate heat in the presence of a radio frequency (RF) field due to their loss mechanisms. Magnetic hyperthermia is a therapeutic concept where magnetic nanoparticles are used as heat generators to kill cancer cells. Specific absorption rate (SAR) is defined as the amount of heat generated by a unit mass of magnetic components in the presence of a RF magnetic field [10,11]. Magnetic particles with a high SAR value are desirable for magnetic hyperthermia, as the amount of dosage required to increase the temperature to the therapeutic limit can be significantly reduced. The SAR value depends on several factors such as the particle size, shape, chemical composition, magnetic properties, particle concentration, RF-field strength and frequency, *etc.* [12,13]. For a controllable hyperthermia, particles with a low Curie temperature are desirable [14].

Cobalt ferrite ($CoFe_2O_4$) is a hard magnetic material with a moderate saturation magnetization and large coercive force. The magnetic properties of cobalt ferrite can be tuned by substitution with nonmagnetic zinc ions. The substitution with zinc ions in the tetrahedral sites of

*E-mail: ilrhee@knu.ac.kr

the inverse spinel structure leads to changes in the magnetic properties of cobalt ferrite owing to the exchange interactions between lattice sites [15,16]. Some studies reported that the zinc-substitution in cobalt ferrite leads to an increase in the saturation magnetization and reduction in coercivity [17]. In addition, the zinc substitution leads to an increase of the chemical stability [18].

In this study, we fabricated polymer-coated cobalt zinc ferrite nanoparticles to modulate their magnetic properties for hyperthermia applications by employing a one-step synthesis technique that does not require further heat treatment for achieving a good crystallinity. The SAR of the nanoparticles was 83 W/g for a low particle concentration of 5 mg/mL, which revealed that the triethylene glycol (TREG)-coated cobalt zinc ferrite nanoparticles are suitable for magnetic hyperthermia applications.

II. EXPERIMENTAL METHODS

All the chemicals for the synthesis of the particles were purchased from Sigma Aldrich, and used without further modification. Deionized water was used throughout the synthesis. TREG-coated zinc doped cobalt ferrite nanoparticles were synthesized using a one-step hydrothermal technique with a 100-mL teflon stainless-steel autoclave. The nanoparticles were coated with TREG during their synthesis. For the synthesis of the TREG-stabilized $Co_{0.6}Zn_{0.4}Fe_2O_4$ particles, 190.34 mg of $CoCl_2{\cdot}6H_2O$, 163.56 mg of $ZnCl_2{\cdot}6H_2O$, and 1 g of $FeCl_3{\cdot}6H_2O$ were dissolved in 20-mL deionized water in a 100-mL beaker through magnetic stirring, followed by the addition of 3 mL of TREG. Using a 0.5-M NaOH solution, pH was adjusted to 11. The color of the mixture turned dark-brown after the addition of the NaOH solution. The mixture was continuously stirred at ambient temperature using a magnetic stirrer under an argon atmosphere, introduced to obtain a homogeneous mixture. Then, the homogenized mixture was transferred into the teflon-lined stainless-steel autoclave with a 40% filling, and kept in a vacuum oven at 160 °C for 12h. Then, the solution was allowed to naturally cool down to room temperature in the vacuum oven. The nanoparticles were separated from the solution using a magnet to discard

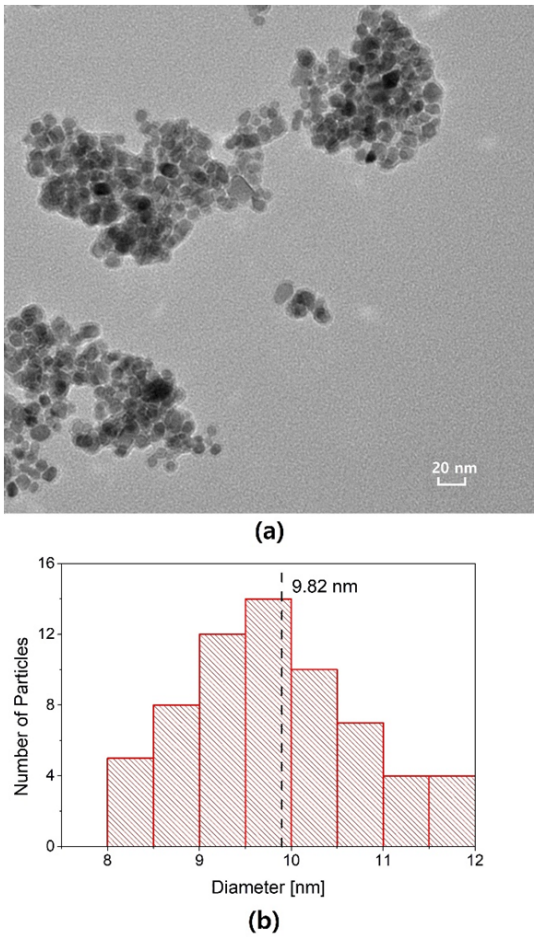

Fig. 1. (Color online) (a) TEM image and (b) particle size distribution of the TREG-coated cobalt zinc ferrite nanoparticles.

the unreacted residue in the solution after the synthesis. This cleaning process was performed several times by redispersing the nanoparticles in water, and then using a magnet to separate the product from the solution until a complete removal of the unreacted products. The particles were redispersed in water for a further characterization.

The crystallinity and inverse spinel structure of the sample were analyzed using X-ray diffraction (XRD; X'pert PRO, PANalytical). The particle shape and size distribution were revealed using transmission electron microscopy (HT 7700, Hitachi Ltd). The stoichiometry of the nanoparticles was analyzed using inductively coupled plasma spectroscopy (ICP; IRISAP, Thermo Jarrell Ash). A vibrating sample magnetometer (VSM; MPMS, Quantum Design) was used to measure the magnetic properties of the particles. A Fourier-transform

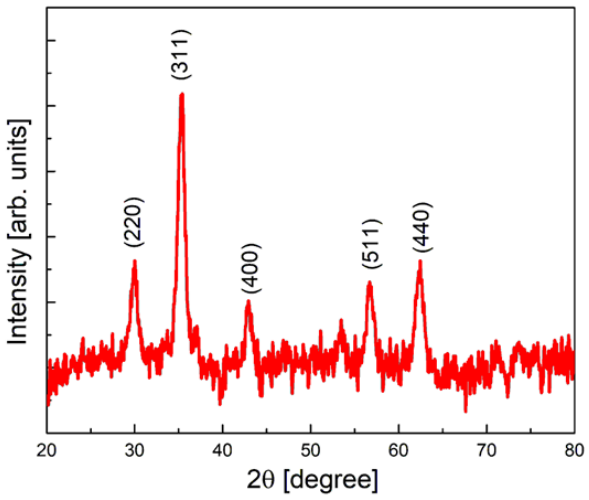

Fig. 2. (Color online) XRD patterns of TREG-coated cobalt zinc ferrite nanoparticles. The indices of the crystal planes in the figure match with those of inverse spinel ferrite.

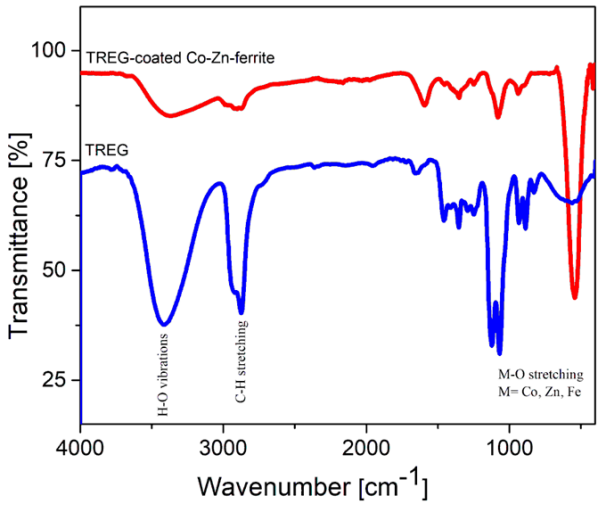

Fig. 3. (Color online) FTIR spectra of pure TREG and TREG-coated cobalt zinc ferrite nanoparticles. The absorption bands correspond to the stretching and vibration modes of specific chemical bonds.

infrared spectrometer (FT-IR; Nicolet 380, Thermo Scientific USA) was used to confirm the TREG-coating on the surface of the particles. Magnetic hyperthermia measurements were performed using an induction heating system (Osung High Tech, OSH-120-B). The temperature of the aqueous solution of particles was measured with a CALEX infrared thermometer (PyroUSB CF, Calex Electronics Limited).

III. RESULTS AND DISCUSSION

X-ray diffraction patterns of the TREG-coated zinc-doped cobalt ferrite nanoparticles are shown in Fig. 1. The plane indices observed in the graph matched with those of the characteristic inverse spinel structure of ferrites [JCPDS no. 22-1086].

A TEM image of the coated particles is shown in Fig. 2. A particle-size distribution histogram is obtained by analyzing one hundred representative particles observed in the TEM image. The particles were spherical, with an average diameter of 9.82 nm.

The status of the TREG-coating on the surface of the particles was checked using FT-IR spectra, recorded in the range of 400∼4000 cm^{-1}, as shown in Fig. 3. The spectra exhibit absorption bands, which are in a good agreement with the characteristic FT-IR spectra of pure TREG and TREG-stabilized cobalt zinc ferrite particles [19]. The C-H stretching at 2800∼2980 cm^{-1} and C-O stretching at 1060∼1080 cm^{-1} revealed the presence of TREG molecules, the coating agent on the particles' surfaces [19]. The broad band around 3400 cm^{-1} is attributed to the stretching vibration of O-H in the hydroxyl groups of the TREG and water molecules at the particles' surfaces. The bands at 2874 cm^{-1} and 2980 cm^{-1} correspond to the characteristic symmetric and asymmetric C-H stretching vibrations of the (-CH_2) methylene groups. The two bands at 1060∼1080 cm^{-1} correspond to the C-O stretching vibration, which confirms the presence of organic molecules on the surfaces of the particles. The two bands in the range of 400∼600 cm^{-1} emerge owing to the metal-oxygen stretching vibration at the octahedral and tetrahedral lattice sites. The bands at 542 cm^{-1} and 415 cm^{-1} correspond to the stretching vibrations of Fe-O and Zn-O, respectively. These bands confirm the TREG coating on the surfaces of the particles [20].

The magnetization of the TREG-coated particles as a function of the applied field at room temperature is shown in Fig. 4. The saturation magnetization of the particles is 84 emu/g, while the coercive force is 32 Oe. The value of the saturation magnetization is larger than previously reported values [15]. The low coercivity and high saturation magnetization of the particles indicate that the TREG-coated particles are a good candidate

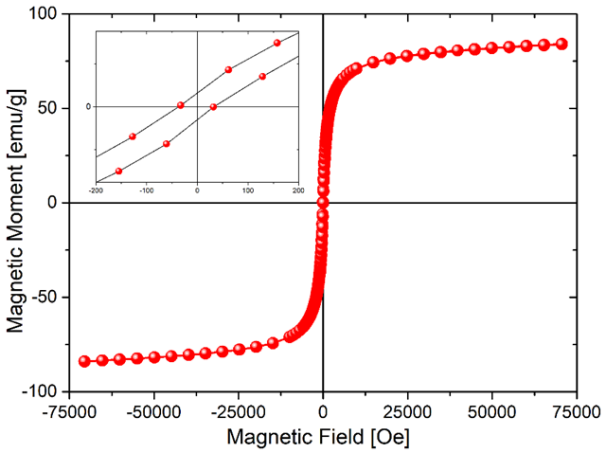

Fig. 4. (Color online) Magnetic moment of the nanoparticles as a function of the applied magnetic field. The particles exhibit a negligible coercive force, as shown in the inset.

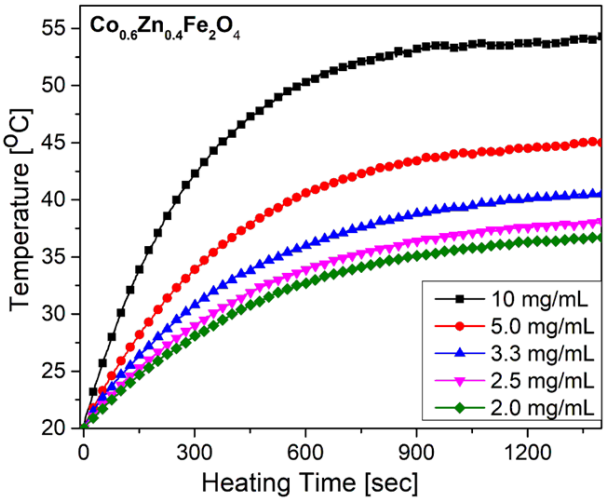

Fig. 5. (Color online) Heating curves of the aqueous solutions of the particles with various concentrations. The temperature initially rapidly increases, and then it saturates after approximately 900 s.

for magnetic hyperthermia applications [21]. The coercive force is small compared with that of the cobalt ferrite nanoparticles [22], most likely owing to the decrease in magneto-crystalline anisotropy caused by the zinc doping. Similar results have been reported in Ref. [23].

Calorimetric measurements were performed to evaluate the heating efficiency of nanoparticles in the presence of an AC magnetic field. An induction heating system and an IR temperature sensor were employed to obtain the heating curves as a function of the time, as shown in Fig. 5 for the aqueous samples with five different particles concentrations. The samples were measured in the

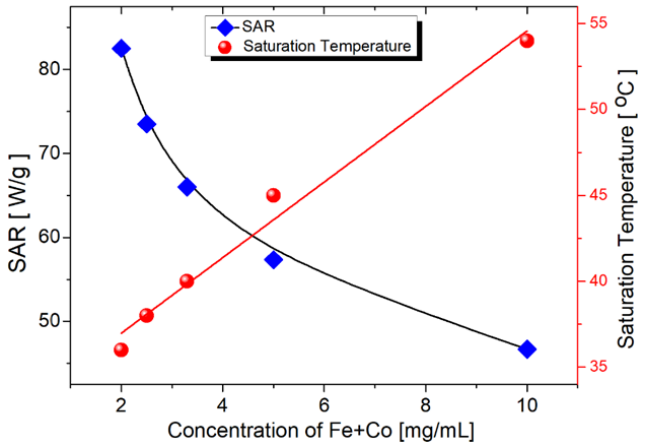

Fig. 6. (Color online) Concentration dependence of the SAR and saturation temperature. The optimal concentration of particles in an aqueous solution for a target temperature of 42 °C is 4.58 mg/mL.

presence of an alternating field with a strength of 4.5 kA/m and frequency of 216 kHz. The temperature of the samples initially rapidly increased, and then it saturated within approximately 900 s, when the heat generation of the particles was balanced with the heat loss to the environment. The saturation temperature of the 5-mg/mL sample was 45 °C, higher than the target temperature for hyperthermia applications of 42 °C. The target temperature can be achieved by controlling the particle concentration in the aqueous solution. The dependences of the saturation temperature and SAR as a function of the particles concentration are shown in Fig. 6. With a particles concentration of 4.58 mg/mL, the target temperature of 42 °C can be achieved.

SAR is defined as the generated heat per unit mass of the magnetic constituents in the particles; it can be expressed in W/g. When the particles are dispersed in an aqueous solution, the SAR is [24]:

$$SAR = \sum c_W \frac{m_W}{m_{Co+Fe}} \frac{dT}{dt}, \qquad (1)$$

where, c_W is the specific heat of water (4.18 J·g^{-1}·K^{-1}), $\frac{dT}{dt}$ is the initial temperature increase of the heating curve, and m_{co+Fe} is the mass of the magnetic components (cobalt and iron) in the sample which is determined using inductively coupled plasma spectroscopy.

The heating efficiency of nanoparticles is mainly determined by two types of loss mechanisms, hysteresis loss in multi-domain nanoparticles and relaxation losses in

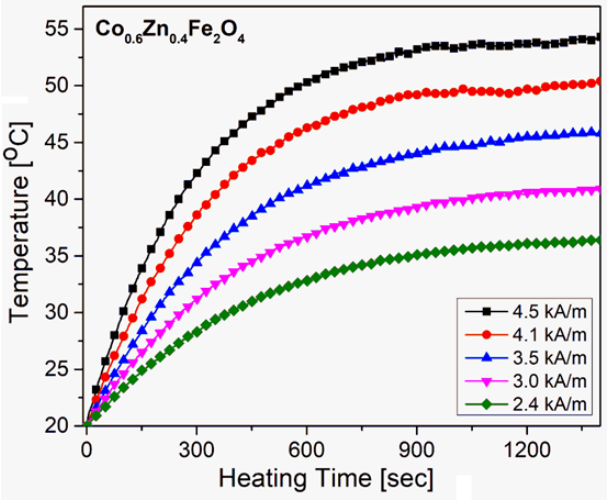

Fig. 7. (Color online) Field-strength dependence of the heating curves for the 10-mg/mL sample. The saturation temperature increases with the field strength.

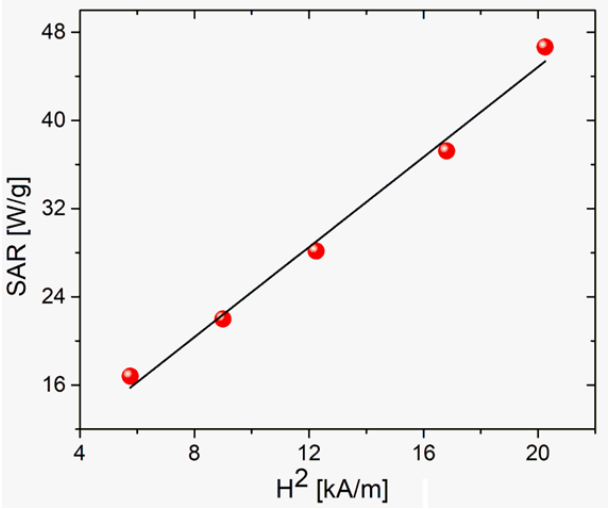

Fig. 8. (Color online) Dependence of the SAR as a function of the square of the field strength. These data are consistent with Eq. (2).

superparamagnetic nanoparticles. In our case, the coercive force is very small; therefore, we can ignore the heat contribution of the hysteresis loss during temperature increase. The relaxation losses are divided into Néel loss, caused by the rotation of the magnetic moment in the presence of an alternating magnetic field, and Brownian loss, caused by the physical rotation of the nanoparticles in the aqueous media. Therefore, both saturation magnetization and particle size are important factors that determine the SAR [25].

The concentration dependence of the SAR is shown in Fig. 6. The 2-mg/mL sample showed the largest SAR value of 83 W/g; the SAR decreased with the increase of the particles concentration. This behavior can be explained through the dipolar interactions [24, 26]. The separation between particles decreases with the increase of the particles concentration, which leads to enhanced dipolar interactions between particles, which in turn reduces the Néel loss [27].

The effect of the field strength on the heating of the particles was also evaluated. The heating curves for field strengths in the range of 2.4∼4.5 kA/m are shown in Fig. 7. The frequency was fixed to 216 kHz. The power loss in the magnetic particles as a function of the applied field strength is [28]:

$$P = \frac{1}{2}\mu_0\chi''\omega H_0^2, \qquad (2)$$

where, H_0 and ω are the strength and angular frequency of the alternating magnetic field, while χ'' is the magnetic susceptibility of the particles, which depends on the Néel and Brownian relaxation times of the particles. The SAR is proportional with the power loss expressed by Eq. (2). Fig. 8 shows that there is a linear relationship between the SAR and H_0^2, as expected.

IV. CONCLUSION

Zinc-doped cobalt ferrite nanoparticles were fabricated using a one-step hydrothermal synthesis method and characterized for magnetic hyperthermia applications. This hydrothermal route is cost effective and highly reproducible. X-ray diffraction measurements confirmed the inverse spinel structure of the particles that were spherical with an average diameter of 9.82 nm. The presence of a TREG coating on the surfaces of the particles was confirmed from the FT-IR spectra. The particles were superparamagnetic with a negligible coercive force. In addition, the particles exhibited a high SAR in an aqueous solution owing to their high saturation magnetization. The optimal concentration of particles for achieving the target hyperthermia temperature of 42 °C was 4.58 mg/mL. The linear relationship between the SAR and the square of field strength was also confirmed. These findings show that the TREG-coated cobalt zinc ferrite nanoparticles are suitable for magnetic hyperthermia applications.

ACKNOWLEDGEMENTS

This research was supported by the National Research Foundation of Korea (2016R1A2B1006449).

REFERENCES

[1] O. Masala and R. Seshadri, J. Am. Chem. Soc. **127**, 9354 (2005).
[2] K. Mukherjee, D. Bharti and S. Majumder, Sens. Actuators B: Chem. **146**, 91 (2010).
[3] E. Brück, J. Phys. D: Appl. Phys. **38**, R381 (2005).
[4] T. Ahmad, H. Bae, Y. Iqbal, I. Rhee and S. Hong *et al.*, J. Magn. Magn. Mater. **381**, 151 (2015).
[5] J.-H. Lee, Y.-M. Huh, Y.-W. Jun, J.-W. Seo and J.-T. Jang *et al.*, Nat. Med. **13**, 95 (2007).
[6] D. H. Kim, H. Zeng, T. C. Ng and C. S. Brazel, J. Magn. Magn. Mater. **321**, 3899 (2009).
[7] Q. A. Pankhurst, J. Connolly, S. K. Jones and J. Dobson, J. Phys. D: Appl. Phys. **36**, R167 (2003).
[8] A. Ahmad, H. Bae, I. Rhee and S. Hong, J. Magn. Magn. Mater. **447**, 42 (2018).
[9] R. Hergt, R. Hiergeist, I. Hilger, W. A. Kaiser and Y. Lapatnikov *et al.*, J. Magn. Magn. Mater. **270**, 345 (2004).
[10] R. Epherre, E. Duguet, S. Mornet, E. Pollert and S. Louguet *et al.*, J. Mater. Chem. **21**, 4393 (2011).
[11] I. Rhee, New Phys.: Sae Mulli **65**, 411 (2015).
[12] H. Hergt, S. Dutz and M. Röder, J. Phys. Condens. Matter **20**, 385214 (2008).
[13] F. Shubitidze, K. Kekalo, R. Stigliano and I. Baker, J. Appl. Phys. **117**, 094302 (2015).
[14] E. Pollert, K. Knížek, M. Maryško, S. Kašpar and S.Vasseur *et al.*, J. Magn. Magn. Mater. **316**, 122 (2007).
[15] H. Sozeri, Z. Durmus and A. Baykal, Mater. Res. Bull. **47**, 2442 (2012).
[16] S. Urcia-Romero, O. Perales-Pérez, O. Uwakweh, C. Osorio and H. A. Radovan, J. Appl. Phys. **109**, 07B512 (2011).
[17] G. V. Duong, N. Hanh, D. V. Linh, R. Groessinger and P. Weinberger *et al.*, J. Magn. Magn. Mater. **311**, 46 (2007).
[18] G. Vaidyanathan and S. Sendhilnathan, Physica B Condens Matter **403**, 2157 (2008).
[19] J. Wan, X. Jiang, H. Li and K. Chen, J. Mater. Chem. **22**, 13500 (2012).
[20] R. D. Waldron, Phys. Rev. **99**, 1727 (1955).
[21] M. Veverka, K. Závěta, O. Kaman, P. Veverka and K. Knížek *et al.*, J. Phys. D: Appl. Phys. **47**, 065503 (2014).
[22] R. Topkaya, A. Baykal and A. Demir, J. Nanopart. Res. **15**, 1359 (2013).
[23] V. Mameli, A. Musinu, A. Ardu, G. Ennas and D. Peddis *et al.*, Nanoscale **8**, 10124 (2016).
[24] Y. Iqbal, H. Bae, I. Rhee and S. Hong, J. Magn. Magn. Mater. **409**, 80 (2016).
[25] M. Ma, Y. Wu, J. Zhou, Y. Sun and Y. Zhang *et al.*, J. Magn. Magn. Mater. **268**, 33 (2004).
[26] A. E. Deatsch and B. A. Evans, J. Magn. Magn. Mater. **354**, 163 (2014).
[27] J. Dormann, L. Bessais and D. Fiorani, J. Phys. C: Solid State Phys. **21**, 2015 (1988).
[28] R. E. Rosensweig, J. Magn. Magn. Mater. **252**, 370 (2002).